Check for updates

Blue to magenta tunable luminescence from LaGaO$_3$: Bi^{3+}, Cr^{3+} doped phosphors for field emission display applications†

Ch. Satya Kamal,[ab] T. K. Visweswara Rao,[a] T. Samuel,[a] P. V. S. S. S. N. Reddy,[a] Jacek B. Jasinski,[c] Y. Ramakrishna,[d] M. C. Rao[e] and K. Ramachandra Rao [ID] *[ac]

A series of blue to magenta emitting color-tunable LaGaO$_3$: Bi^{3+}/Cr^{3+} phosphors were prepared by chemical routes, and their phase structure, morphology and photoluminescence (PL) properties were investigated in detail. Luminescence studies indicated that the optimum concentrations of Bi^{3+} and Cr^{3+} in LaGaO$_3$ were found to be 1 at% and 3 at%. Co-doping with Bi^{3+} ions resulted in increased Cr^{3+} emission intensity and gradual reduction in Bi^{3+} emission intensity, confirming the presence of a Bi^{3+}–Cr^{3+} energy transfer. The energy transfer (ET) mechanism from the host lattice to the Bi^{3+} and Cr^{3+} ions in the LaGaO$_3$: Bi^{3+}/Cr^{3+} phosphor has been explained. The ET efficiency has been calculated and found to be 55%. The critical ET distance has been calculated by the concentration-quenching method. The enhanced intensity and tuned luminous color of LaGaO$_3$: Bi^{3+}/Cr^{3+} phosphors provided a promising material for field emission display devices.

Introduction

Currently, oxide-based perovskite phosphors are strategic components for display applications, described by the general chemical formula ABO$_3$. Research on these materials opens a variety of new possibilities in the field of flat panel display devices, which can be integrated into various types of displays such as plasma display panels (PDPs), vacuum fluorescent displays (VFDs), electro-luminescent displays (EDs) and field emission displays (FEDs).[1–7] In comparison to conventional phosphors for cathode ray tubes (CRT), it is important to develop phosphors for display devices that show high efficiency and good stability at low-voltage electron excitation and high current density.[5–9] Therefore, selection of suitable phosphors material is considered to be one of the most critical and urgent challenges in the lighting field. It is well known that besides from its luminescence applications, LaGaO$_3$ perovskite have been promising material as an electrolyte for solid fuel cells.[10,11] The lanthanum gallate (LaGaO$_3$) crystal has an orthorhombically distorted centrosymmetric GdFeO$_3$ type perovskite-like

structure with space group *Pbnm*.[12] Indeed, LaGaO$_3$ is a relatively simple matrix, which consists three dimensional sublattice of corner connected GaO$_6$ octahedra and the La^{3+} is in eight-fold coordination with oxygen ions, and is potentially act as a host material in phosphor applications. LaGaO$_3$ doped with several rare earth (RE) ions (RE = Eu, Tb, Dy/Eu, Sm/Tb *etc.*) were extensively studied for their luminescence properties, color rendering properties and superior stability under electron bombardment.[13–15] The luminescent properties of Bi^{3+} doped LaGaO$_3$ were studied by B. Jacquier *et al.*[16] reported that Bi^{3+} was a good activator of luminescence for lanthanide compounds having its transitions between the ground state $^1S_0$ and the excited levels $^3P_1$ and $^1P_1$. Alok M. Srivastava *et al.*[17] reported thermal quenching of Bi^{3+} luminescence in LaGaO$_3$ and explained the energy transfer mechanism between Bi^{3+} ions to host lattice-quenching centers. Research reports also show that along with Eu^{2+}, Ce^{3+}; Bi^{3+} could be used as sensitizer ion to produce abundant and tunable emission colors including white *via* adjusting doped ion concentrations.[18–22] Trivalent chromium (Cr^{3+}) is widely used as a luminescent dopant in various materials. Chromium is a low-cost activator, which can provide deep red color and bright luminescence. On this account, Cr^{3+} is the subject of numerous optical spectroscopic, vivo imaging, energy saving and luminescence applications.[23–26] Recently, significant efforts have been devoted by several research groups on the synthesis and characterization of various Cr^{3+} doped host materials.

Our present studies have paid more attention to investigate NIR photoluminescence of Cr^{3+} ions doped LaGaO$_3$ phosphors and also including the enhancement in intensity of Cr^{3+} ions on

[a]Crystal Growth and Nano-Science Research Center, Department of Physics, Government College (A), Rajamahendravaram, Andhra Pradesh, India-533105. E-mail: drkrcr@gmail.com

[b]Department of Physics, Adikavi Nannaya University, Rajamahendravaram, Andhra Pradesh, India

[c]Conn Center for Renewable Energy Research, University of Louisville, KY, USA

[d]Department of Engineering Physics, Andhra University, Visakhapatnam, India

[e]Department Physics, Andhra Loyola College, Vijayawada, AP, India

† Electronic supplementary information (ESI) available. See DOI: 10.1039/c7ra08864g

co-doping with Bi^{3+} ions in detail. To the best of author's knowledge, no accurate information is available on the energy transfer (ET) mechanism and efficiency from Bi^{3+} to Cr^{3+} in $LaGaO_3$ compound. From CIE color coordinates, it is demonstrated that, by carefully selecting Bi^{3+} and Cr^{3+} contents, the relative intensity of the different emissions can be changed producing an overall emission colour that can be tuned from blue to magenta.

Experimental details

Preparation of the nanoparticles

The $LaGaO_3$ undoped, $LaGaO_3$: (0.1, 0.5, 1, 2 at%) Bi^{3+}, $LaGaO_3$: (0.5, 1, 3, 5 at%) Cr^{3+} and $LaGaO_3$: (1 at%) Bi^{3+}, (0.5, 1, 3, 5 at%) Cr^{3+} phosphors were all prepared by the polyol mediated method. Stoichiometric amounts of $La(NO_3)_3 \cdot 6H_2O$ (Sigma-Aldrich, 99.99%), $Ga(NO_3)_3 \cdot H_2O$ (Sigma-Aldrich, 99.99%), $Bi(NO_3)_3 \cdot 5H_2O$ (Sigma-Aldrich, 99.99%), $Cr(NO_3)_3 \cdot 9H_2O$ (Alfa Aesar 98.5%) are used as precursors. Ethylene glycol (MERCK, 99.99%) was used as a solvent and stabilizing ligand. For preparing the undoped lanthanum gallate ($LaGaO_3$), initially stoichiometric amounts of $La(NO_3)_3 \cdot 6H_2O$ and $Ga(NO_3)_3 \cdot H_2O$ was transferred into a two-necked RB flask containing solution of 20 ml ethylene glycol. The solution was kept under magnetic stirring and continuous heating. When the temperature was at 100 °C, around 2 gram urea was added and temperature was raised further to 120 °C and kept up at this temperature for 2 hours. The formed precipitate was cooled, centrifuged, washed thrice with methanol, twice with acetone and allowed to dry overnight at room temperature. Then the samples were sintered in a muffle furnace at a temperature of 1000 °C for 5 h. Finally, the samples are naturally cooled down to room temperature and fully ground for further investigations. The above procedure was repeated for the preparation of Cr and Bi/Cr, doped $LaGaO_3$ samples by dissolving required amount of $Cr(NO_3)_3 \cdot 9H_2O$, and $Bi(NO_3)_3 \cdot 5H_2O$ salts in ethylene glycol.

Characterization

X-ray diffraction (XRD) studies were carried out using a Philips powder X-ray diffractometer (model PW 1071) with Ni filtered Cu-Kα radiation. For calibration purpose, diffraction peak corresponding to the (111) plane of Si at a 2θ value of 28.442° was employed. The lattice parameters were obtained from refinement of the XRD patterns using POWDERX software. All steady-state luminescence and lifetime measurements were carried out at room temperature using an Edinburgh Instrument (FLSP 920 system) having a 450 W Xe lamp. A microsecond flash lamp and a nanosecond hydrogen flash lamp were used for lifetime measurements. All emission and excitation measurements were carried out with a resolution of 3 nm. Emission spectra were corrected for the detector response and excitation spectra for the lamp profile. The fundamental structural morphologies of the samples and the elemental composition investigation has been done by utilizing a field emission scanning electron microscope FE-SEM Supra 55 (Carl Zeiss, Germany). An

accelerating voltage of 20 kV and magnification of 10k× was used for recording the micrographs.

Results & discussion

Phase formation and microstructure

Fig. 1(a) shows the XRD patterns of undoped $LaGaO_3$, $LaGaO_3$: 1 at% Bi^{3+}, $LaGaO_3$: 3 at% Cr^{3+} and $LaGaO_3$: 1 at% Bi^{3+}, 3 at% Cr^{3+}
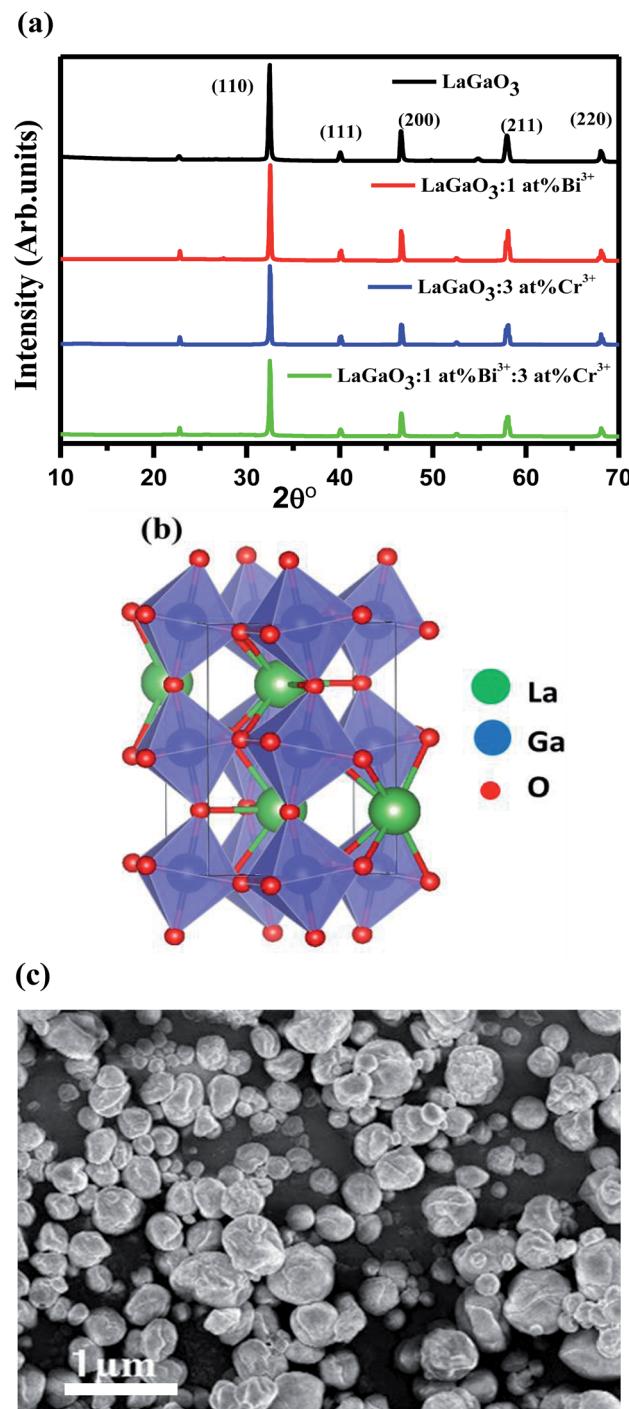
Fig. 1 (a) XRD patterns of $LaGaO_3$, $LaGaO_3$: Bi^{3+}, $LaGaO_3$: Cr^{3+}, $LaGaO_3$: Bi^{3+}, Cr^{3+} samples (b) 3D crystal structure of $LaGaO_3$ and (c) FE-SEM image of $LaGaO_3$: (1 at%) Bi^{3+}, (3 at%) Cr^{3+} sample.

phosphors. From Fig. 1(a), all the diffraction peaks are in good agreement with the reported orthorhombic phase of $LaGaO_3$ (PCPDF89-7946)[19] and no second phase was detected indicating that the Bi^{3+} and Cr^{3+} completely dissolved in the $LaGaO_3$ host lattice. Table 1 shows lattice parameters and unit cell volume calculated from the peak position of XRD patterns from the

Table 1 Lattice parameters of $LaGaO_3$, $LaGaO_3$: 1 at% Bi^{3+}, $LaGaO_3$: 3 at% Cr^{3+} and $LaGaO_3$: 1 at% Bi^{3+}: 3 at% Cr^{3+} phosphors

| Compositions	a (Å)	b (Å)	c (Å)	V^3 (Å)
$LaGaO_3$	5.478	5.594	7.659	234.70
$LaGaO_3$: 1 at% Bi^{3+}	5.468	5.552	7.691	233.48
$LaGaO_3$: 3 at% Cr^{3+}	5.483	5.617	7.652	235.66
$LaGaO_3$: 1 at% Bi^{3+}, 3 at% Cr^{3+}	5.473	5.563	7.644	232.73
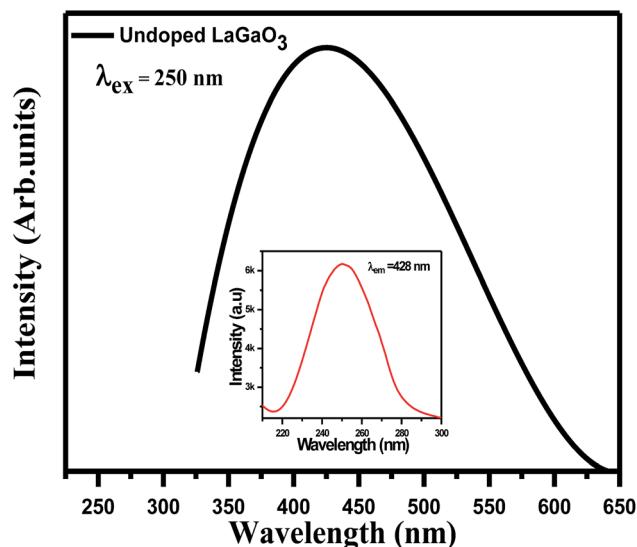
Fig. 2 Emission spectra and excitation (inset) of $LaGaO_3$ phosphor.

undoped and doped $LaGaO_3$ samples whereas average particle size where calculated from the peak width (*i.e.* FWHM) of the most intense peak (110) at $2\theta = 32.49°$ from the XRD pattern using Scherrer's equation ($D = 0.9\lambda/\beta \cos\theta$, where D is the average particle size, λ is the wavelength of X-rays and β is the corrected full width at half maximum (FWHM) of an observed peak). The average crystallite size (D) of pure $LaGaO_3$, doped and co-doped $LaGaO_3$ particles which are annealed at 1000 °C are estimated in the range of 70–80 nm. $LaGaO_3$ structure shown in Fig. 1(b) consists of slightly distorted and tilted GaO_6 octahedra are linked to each other by corner sharing to form three-dimension network and the La^{3+} is in eight-fold coordination with oxygen ions. The average bond length of Ga–O in GaO_6 is 1.975 Å; while La^{3+} is 8-coordinated by O atoms with average bond length of 2.62 Å for La–O. The minor changes in lattice parameters of single doped Bi^{3+}, Cr^{3+} and co-doped in $LaGaO_3$ when compared with undoped $LaGaO_3$ depends on ionic radii.[22] The radius of Bi^{3+} ($r = 1.03$ Å, coordination number, CN = 6) is similar to that of La^{3+} ($r = 1.16$ Å, CN = 8), while the radius of Cr^{3+} ($r = 0.61$ Å, CN = 6) is comparable to that of Ga^{3+} ($r = 0.47$ Å, CN = 6),[27] thus in Bi^{3+}–Cr^{3+} co-doped $LaGaO_3$, Bi^{3+} mostly likes to take La site and Cr^{3+} likes to take Ga site. SEM image of the selected $LaGaO_3$: 1 at% Bi^{3+}, 3 at% Cr^{3+}+ phosphor is presented in Fig. 1(c). It is clearly seen that the sample is composed of aggregated particles with size ranging from 60 to 90 nm. The approximate spherical morphology and particles size confirms that these phosphors can be used potentially in the future field emission display device applications.

Photoluminescence and energy transfer (ET) mechanism of the samples

Excitation (inset) and emission spectra of host $LaGaO_3$ at room temperature shown in Fig. 2, with excitation at 250 nm, host $LaGaO_3$ gives a wide band from 300 to 600 nm with a maximum peak at 428 nm, which is attributed to the transition of self-
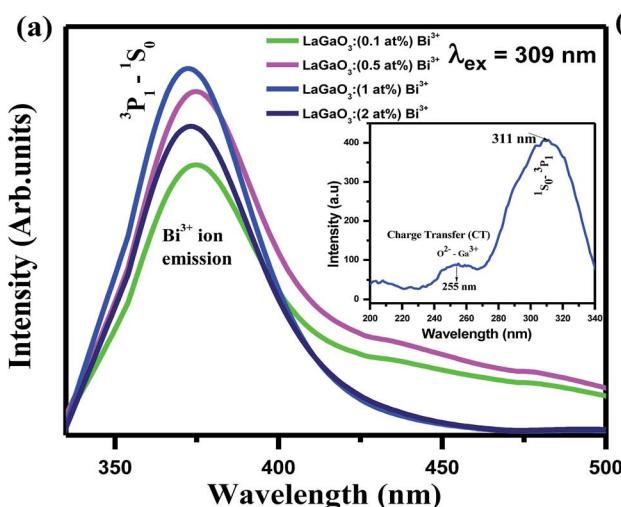
Fig. 3 (a) Emission spectra and excitation (inset) spectra of $LaGaO_3$: Bi^{3+} phosphor (b) decay curve for $LaGaO_3$: Bi^{3+} phosphor excited at 309 nm and monitored at 374 nm.
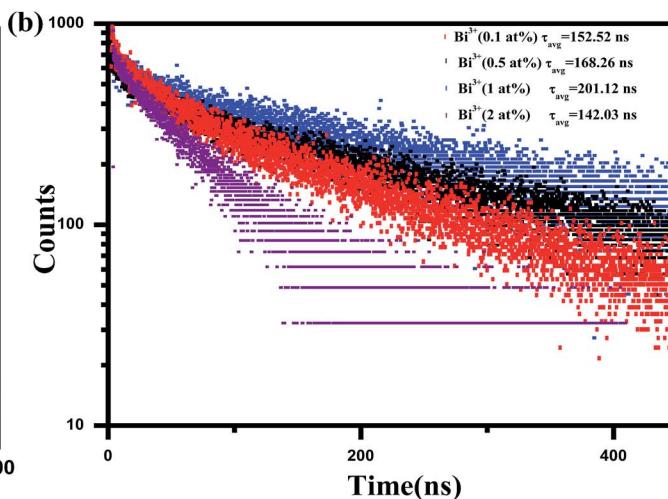
activated optical center corresponding to groups in the host lattice GaO_6.[28] Monitored at 428 nm (inset), the corresponding excitation spectra in the range of 200–300 nm is observed with maximum peak position at 428 nm.

The excitation (inset) and emission spectra of a samples $LaGaO_3$: (0.1, 0.5, 1, 2) at% Bi^{3+} is shown in Fig. 3(a), it is observed that the emission band centred at ~374 nm which is attributed to $^3P_1$–$^1S_0$ transition of Bi^{3+} ion on excitation with 309 nm.

With increasing Bi^{3+} concentration, the intensity of the 374 nm emission band increases and reaches a maximum at 1 at% and decreases when Bi^{3+} content is further increased due to concentration quenching effect. Hence, multiphonon relaxation and the cross relaxation between neighboring Bi^{3+} ions, substantially quench the photoluminescence.[29] Hence, the optimized Bi^{3+} content is at $x = 1$ at%. This is also confirmed from the corresponding bi-exponential lifetime decay values (152.52 ns, 168.26 ns, 201.12 ns, 142.03 ns) and curves of Bi^{3+} ions in $LaGaO_3$ which is shown in Fig. 3(b)[30] (procedure for calculation of decay values shown in preceding sections).

The excitation spectra shows weak band around 255 nm due to the charge transfer (CT) transition of 2p orbital of O^{2-} to the empty 4s orbital of Ga^{3+} because the 3d orbital is completely filled[31] and another is at 309 nm due to $^1S_0$–$^3P_1$ electron transition of Bi^{3+} ion respectively. And overlapping of the absorption band of $^1S_0$–$^1P_1$ state of Bi^{3+} ions and the (O–Ga) CT transition is also observed.[16] Emission band of host $LaGaO_3$ is found to overlap with excitation band of $LaGaO_3$: 1 at% Bi^{3+} phosphor in the range of 275–350 nm, so, energy transfer (ET) between Bi^{3+} ion and GaO_6 group may be formed shown in Fig. 1S.† In addition, it is worth to note that $LaGaO_3$: 1 at% Bi^{3+} phosphor with excitation around 309 nm does not show host emission band assigned to Ga^{3+}–O^{2-} transition because the excited electrons in GaO_6 group directly transfer the energy from the conduction band level of GaO_6 to higher excited level of Bi^{3+} ion by energy transfer process.

Fig. 4(a and b) shows the emission and excitation spectra of $LaGaO_3$: (0.5, 1, 3, and 5 at%) Cr^{3+} phosphor. Under excitation at 453 nm, the sample exhibits a broadening $^2E \rightarrow {}^4A_2$ emission peaking at 740 nm ranging from ~650 to 800 nm. The broadening of the $^2E \rightarrow {}^4A_2$ emission is possibly caused by the electron-phonon coupling in the host lattice. The excitation spectrum shown in Fig. 4(b) monitored at 740 nm covers a very broad spectra ranging from 200 to 700 nm and consists of three excitation bands originating from the d–d inner transitions of Cr^{3+}, i.e., 262 nm band originating from the $^4A_2 \rightarrow {}^4T_1$ (te^2) transition, the 453 nm band originating from the $^4A_2 \rightarrow {}^4T_1$ (t^2e) transition and the 617 nm band originating from the $^4A_2 \rightarrow {}^4T_2$ ($t^2e/^2E$) transition.[32,33] In addition to this, (Fig. 4(a) inset) shows the variation in the Cr^{3+} concentration-dependent PL intensities, and the optimum doping concentration was found at $y = 3$ at%.

After that, the PL intensity begins to reduce owing to the concentration quenching effect of Cr^{3+} ions. Furthermore, a schematic diagram of the related energy levels for $LaGaO_3$: Cr^{3+} phosphors is depicted in energy level diagram Fig. 4(c). As for the photoluminescence process, under light excitation
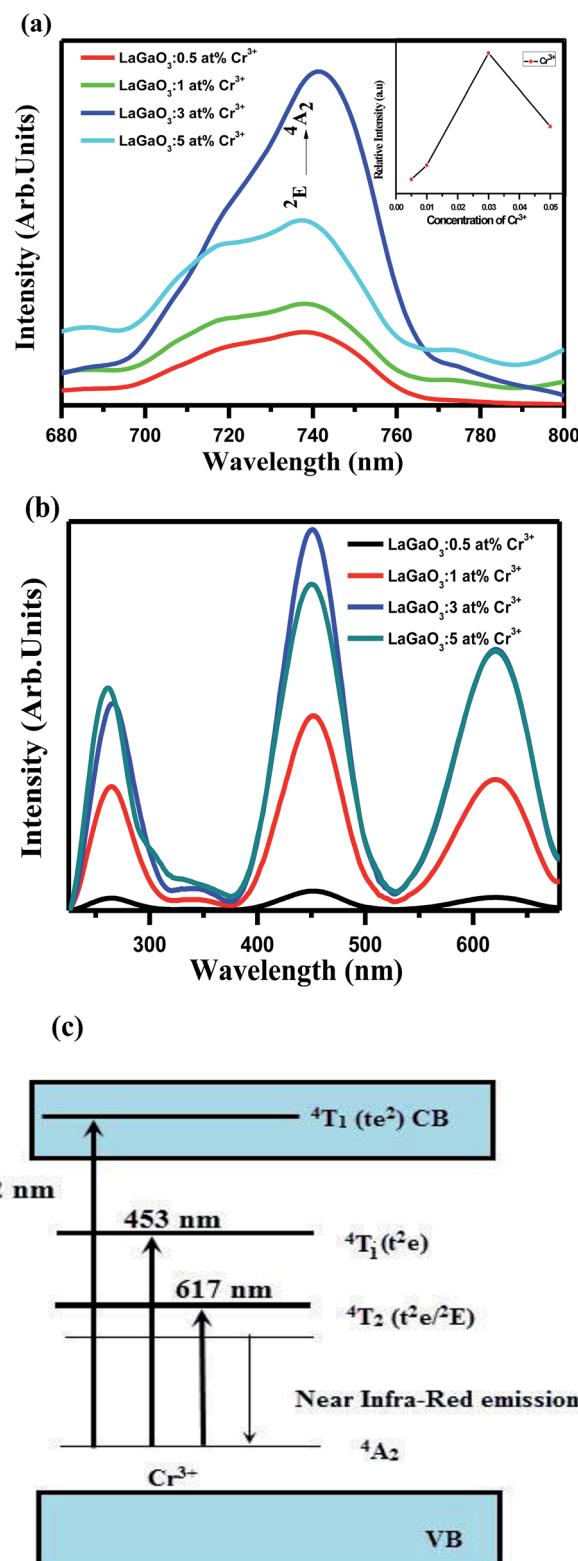
Fig. 4 (a) Emission spectra (inset: PL intensity dependence on Cr^{3+} content) (b) excitation spectra of $LaGaO_3$: Cr^{3+} phosphor excited at 453 nm and monitored at 740 nm. (c) Schematic diagram of the photoluminescence showing the excitation, electron transitions of Cr^{3+} in $LaGaO_3$: Cr^{3+} phosphor.

corresponding to different wavelength, such as 261 nm, the ground-state electrons of Cr^{3+} ions are promoted to the $^4T_1$ (te^2) level. The excited electrons will relax to the ^2E energy level, and shows the near Infra-Red emission *via* the $^2E \rightarrow {}^4A_2$ transition. The corresponding bi-exponential average lifetime decay values and curves of Cr^{3+} ions (1.48 ms, 3.26 ms, 3.91 ms, 2.14 ms) in $LaGaO_3$ which is shown in Fig. 5. The efficient ET needs to have a significant spectral overlap between the emission bands of undoped and Bi^{3+} doped $LaGaO_3$, Fig. 2S† to excitation bands of $LaGaO_3$: 3 at % Cr^{3+} nanophosphor, in the range of 250–800 nm. Thus it can be speculated that in the co-doped $LaGaO_3$, the energy transfer from GaO_6 to Cr^{3+} and Bi^{3+} to Cr^{3+} may occur.

In Fig. 6(a), it is observed that the emission spectrum of $LaGaO_3$: 1 at% Bi^{3+}, (0.5, 1, 3, 5 at%) Cr^{3+} contains both Bi^{3+} emission and Cr^{3+} emission when excited at 309 nm. When Bi^{3+} concentration was fixed at 1 at%, and varying the Cr^{3+} concentration, the emission intensity of Cr^{3+} reaches maximum upto 3 at% and then notably decrease of Cr^{3+} emissions is observed on increasing further concentration, which can be rationalized as concentration quenching. From the excitation spectra (inset) (monitored at 740 nm) Fig. 6(a), broad band ranging from (200–400 nm) peak maximum at ∼309 nm is observed which is due to Bi^{3+} ion absorption and peaks around (weak) ∼260 nm, (broad) ∼453 nm are due to d–d transitions of Cr^{3+} ions. Meanwhile, Bi^{3+} emission decreases gradually, and this phenomenon ascribed to energy transfer happened between Bi^{3+}–Cr^{3+} in this system. The relative emission intensities of Cr^{3+} ions at 740 nm and Bi^{3+} ions at 374 nm as a function of Cr^{3+} concentration were shown in Fig. 6(b). In addition it is observed that on excitation with 309 nm along with Bi^{3+}, Cr^{3+} characteristic emissions there is weak host emission around ∼450 nm which is due to GaO_6 transitions, which is overlapped with Bi^{3+} ion emission as shown in (Fig. 6(a)). Since the emission band of the $LaGaO_3$ host overlaps with the excitation band of Bi^{3+}, Cr^{3+} ions, the excited electron gets transfer their energy from GaO_6 group directly to
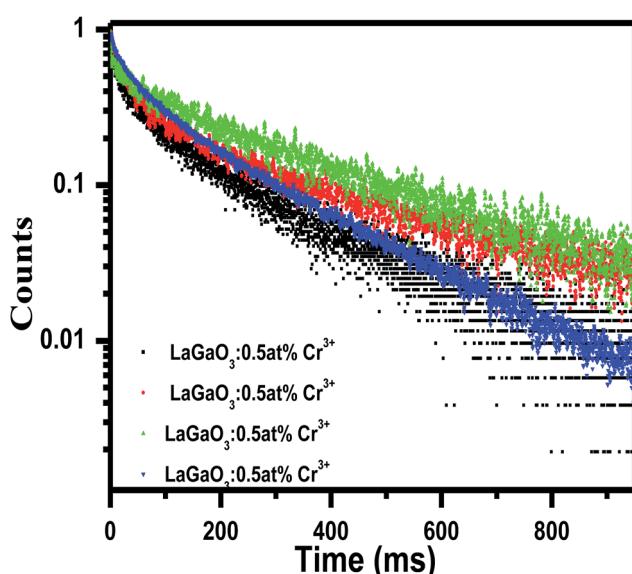

Fig. 5 Average Life time decay curve and values for $LaGaO_3$: Cr^{3+} phosphor excited at 453 nm and monitored at 740 nm.
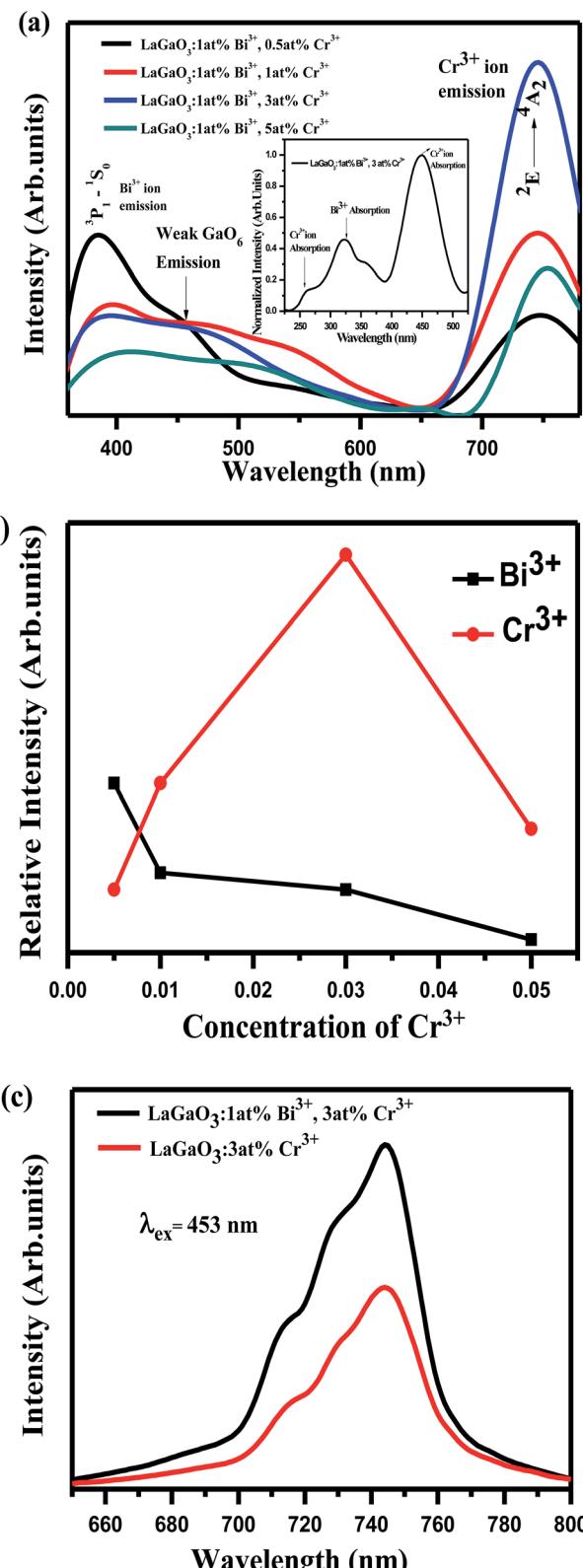

Fig. 6 (a) Emission and excitation (inset) spectra of $LaGaO_3$: 1 at% Bi^{3+}, 3 at% Cr^{3+} phosphor (b) intensity variation of Bi^{3+} as a function of Cr^{3+} concentration (c) intensity enhancement of Cr^{3+} ions on Bi^{3+} co-doping *via* energy transfer between Bi^{3+}–Cr^{3+}.

Cr^{3+} and Bi^{3+} ions. Later, the excited electrons in Bi^{3+} ion then relaxes where some part of energy has been released in the form of 374 nm light and the other part was contributed by the energy transfer process from Bi^{3+} to the Cr^{3+}.

At the same time, we also illustrated the emission profiles (λ_{ex} = 453 nm) of Cr^{3+} ion with and without Bi^{3+} ion presence in host for verifying the intensity enhancement in Cr^{3+} emissions due to Bi^{3+}–Cr^{3+} energy transfer shown in Fig. 6(c). The energy transfer from Bi^{3+} to Cr^{3+}, results in the improvement of Cr^{3+} emission, which is also strongly supported by the decrease in the decay behaviour of the Bi^{3+} emission in co-doped samples.

Decay curves of Bi^{3+} with various Cr^{3+} content for the system $LaGaO_3$: 1 at% Bi^{3+}, (0.5, 1, 3, 5 at%) Cr^{3+} are illustrated in Fig. 7(a and b). The decay curves were well fitted with a double-exponential rule according to the following equation:

$$I = A_1 \exp\left(\frac{-t}{\tau_1}\right) + A_2 \exp\left(\frac{-t}{\tau_2}\right) \tag{1}$$

where, I is the luminescence intensity at the time t, τ_1 and τ_2 are two components of the decay time, A_1 and A_2 are constants. According to these parameters, the average decay times of $LaGaO_3$: 1 at% Bi^{3+}, (0.5, 1, 3, 5 at%) Cr^{3+} nanophosphors can be calculated according to the following formula:[34]

$$\tau = \frac{\left(A_1\tau_1^2 + A_2\tau_2^2\right)}{A_1\tau_1 + A_2\tau_2} \tag{2}$$

Decay times (τ) of Bi^{3+} calculated are about 180.12, 153.25, 127.21 and 90.72 ns for Fig. 7(a) $LaGaO_3$: Bi^{3+} (1 at%), (0.5, 1, 3, 5 at%) Cr^{3+} and corresponding to decay times of 2.27, 3.75, 5.48 and 2.55 ms respectively for varying contents of Cr^{3+} Fig. 7(b).

The increase of Cr^{3+} content leads to faster decay of Bi^{3+} emission, which is attributed to ET from Bi^{3+} to Cr^{3+}. The ET efficiency η_T of Bi^{3+}–Cr^{3+} can be calculated using the following equation[35]

$$\eta_T = 1 - \frac{\tau_S}{\tau_{S0}} \tag{3}$$

where τ_S and τ_{S0} represent the lifetime values of sensitizer Bi^{3+} in the presence and absence of Cr^{3+}. The energy-transfer efficiency η_T values from Bi^{3+} to Cr^{3+} for $LaGaO_3$ are tabulated in Table 2. With increasing Cr^{3+} doping concentrations, the energy-transfer efficiency η_T reaches approximately 55%, indicating that the ET from Bi^{3+} to Cr^{3+} is efficient (Table 2). However, it is well-know that the impurities can affect the luminescence properties, but it has the minute influence. Therefore, the interaction type between sensitizers or between sensitizer and activator can be calculated by the following equation[36]

$$\frac{I}{x} = K\left[1 + \beta(x)^{\theta/3}\right]^{-1} \tag{4}$$

where x is the concentration of the activator ions (Bi^{3+} and Cr^{3+} ions), I is the emission intensity, K and β are constants for the same excitation condition for a given host lattice, and θ is a function of multipole–multipole interaction. When the value of θ is 6, 8, or 10, the interaction types correspond to dipole–dipole (d–d), dipole–quadrupole (d–q), and quadrupole–quadrupole (q–q) interactions, respectively. The dependence of $\log(I/x)$ on $\log(x)$ was found to be relatively linear, and it yields a straight line with a slope equal to $\theta/3$, so we can obtain the θ

Table 2 Energy transfer efficiency (η_T) of the $LaGaO_3$: 1 at% Bi^{3+}, 3 at% Cr^{3+} phosphor

Concentration (x)	η (%)
0.5	11
1	24
3	37
5	55
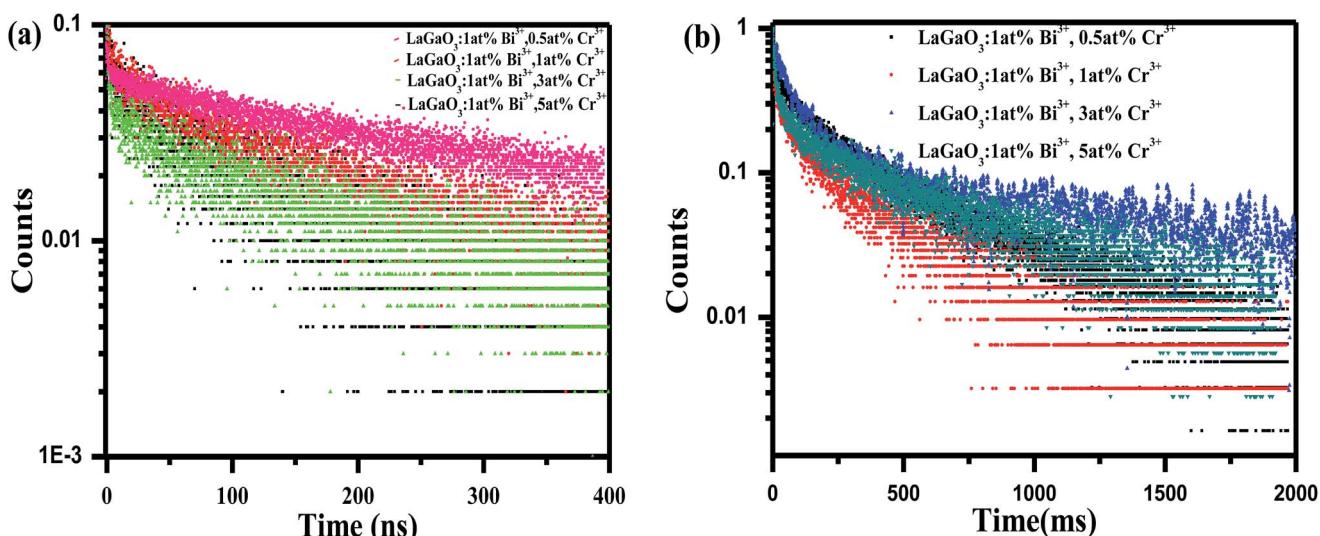
**Fig. 7** (a) Decay curve for Bi^{3+} ions in $LaGaO_3$: 1 at% Bi^{3+}, (0.5, 1,3,5 at%) Cr^{3+} phosphor excited at 309 nm and monitored at 374 nm (b) decay curve for Cr^{3+} ions in $LaGaO_3$: 1 at% Bi^{3+}, (0.5, 1,3,5 at%) Cr^{3+} phosphor excited at 309 nm and monitored at 740 nm.

value to study the energy-transfer process between Bi^{3+} and Cr^{3+} in $LaGaO_3$ host. As shown in Fig. 8 the slope of the straight line is $-\theta/3 = -1.72$ based on the PL data of this series of $LaGaO_3$: 1 at% Bi^{3+}, (0.5, 1, 3, 5 at%) Cr^{3+} samples. The calculated value of θ is 5.16, which is close to six, meaning that the dipole–dipole interaction is the dominant mechanism for the interaction of Bi^{3+} and Cr^{3+} in the $LaGaO_3$ phosphors.

Moreover, the critical distance of Bi^{3+} and Cr^{3+} is also an essential parameter if we consider the concentration quenching effect in this system. We can approximately estimate the critical distance from the report of Blasse, the critical distance (R_c) can be calculated as follows[36]

$$R_c \approx 2\left(\frac{3V}{4\pi X_c Z}\right)^{1/3} \quad (5)$$

where V is the volume of the unit cell, Z represents the number of the activator ions in the unit cell, X_c is about 0.04 from the total concentration of Cr^{3+} (the concentration of 0.03) and Bi^{3+} (the concentration of 0.01). For the $LaGaO_3$ host, the crystallographic parameters are ($V = 244.77$ Å, $Z = 2$). The R_c critical transfer distance is determined to be 11.34 Å. This value is much longer than 5 Å, indicating the possibility of energy transfer via the multipolar interaction mechanism, viz, dipole–dipole interaction as mentioned above.

It is worthwhile to notice that the emission band of Bi^{3+} ions is in blue region and the emission band of Cr^{3+} ions is in red region. Combining both of them, magenta light emission may be achieved. Therefore, the luminescent colors of $LaGaO_3$: Bi^{3+} (1 at%), (0.5, 1, 3, 5 at%) Cr^{3+} phosphors excited by 311 nm are characterized by Commission International de I'Eclairage (CIE) chromaticity diagram and shown in Fig. 9. The Bi^{3+}, Cr^{3+} co-doped samples generates the color tunability from blue to magenta due to an efficient energy transfer from Bi^{3+} to Cr^{3+}. The CIE chromaticity coordinate of $LaGaO_3$: Bi^{3+} 1 at%, 3 at% Cr^{3+} sample is calculated to be (0.45, 0.24), i.e. magenta color is obtained from $LaGaO_3$: Bi^{3+} 1 at%, 3 at% Cr^{3+} sample. The
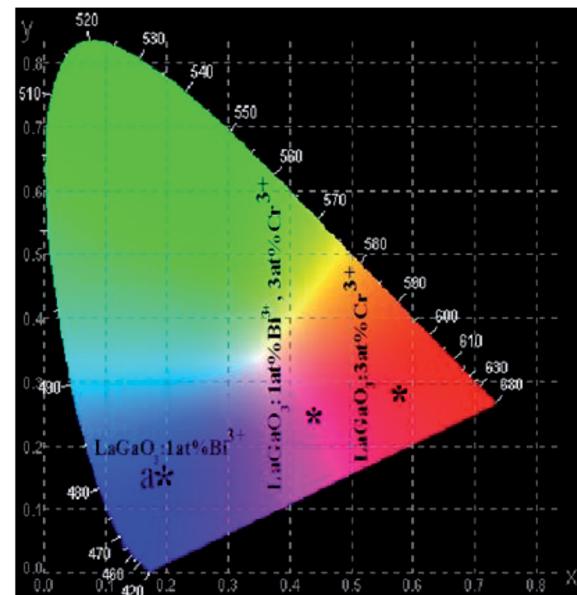

Fig. 9 CIE chromaticity diagram.

results indicate that Bi^{3+}, Cr^{3+} co-doped phosphors may find potential application in field emission display applications.

Conclusions

In this study, Bi^{3+} and Cr^{3+} co-doped $LaGaO_3$ phosphors were prepared by chemical route. XRD proved the orthorhombic phase of $LaGaO_3$: Bi^{3+}, Cr^{3+} phosphors annealed at 1000 °C. The recorded FE-SEM micrograph showed that $LaGaO_3$: Bi^{3+}, Cr^{3+} phosphors were composed of agglomerated and spherical shaped particles. The photoluminescence properties, life time studies and energy transfer process were investigated in detail. The energy transfer from Bi^{3+} to Cr^{3+} was clearly observed and the maximum efficiency found to be 55% from lifetime values. Furthermore, the CIE diagram showed that the colors can be tuned from blue to magenta, indicating that the developed phosphor may potentially be used as a single phase phosphor for field emission display devices.

## Conflicts of interest

There are no conflicts to declare.

Acknowledgements
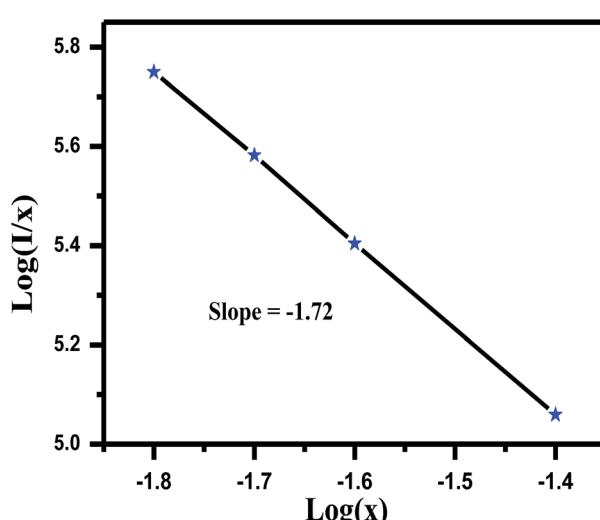
Fig. 8 The fitting line of log (I/x) vs. log(x) in $LaGaO_3$: 1 at% Bi^{3+}, 3 at% Cr^{3+} phosphors beyond the quenching concentration.

Notes and references

1 H. A. Hoppe, *Angew. Chem., Int. Ed.*, 2009, **48**, 3572–3582.

2 I. Shah, *Phys. World*, 1997, **10**, 45–48.

3 B. Chalamala, Y. Wei and B. Gnade, *IEEE Spectrum*, 1998, **35**, 42–51.

4 R. Waser, *Nanoelectronics and Information Technology*, Wiley-Vch, Weinheim, Germany, 2003, ch. 39.

5 C. E. Hunt and A. G. Chakhovskoi, *J. Vac. Sci. Technol., B: Microelectron. Nanometer Struct.–Process., Meas., Phenom.*, 1997, **15**, 516.

6 G. Li and J. Lin, *Chem. Soc. Rev.*, 2014, **43**, 7099.

7 S. S. Pitale, V. Kumar, I. M. Nagpure, O. M. Ntwaeaborwa, E. Coetsee and H. C. Swart, *J. Appl. Phys.*, 2011, **109**, 013105.

8 X. Liu, L. Yan and J. Lin, *J. Electrochem. Soc.*, 2009, **156**(1), 1.

9 S. H. Cho, S. H. Kwon, J. S. Yoo, C. W. Oh, J. D. Lee, K. J. Hong and S. J. Kwon, *J. Electrochem. Soc.*, 2000, **147**, 3143.

10 M. I. Martinez-Rubio, T. G. Ireland, G. R. Fern, J. Silver and M. J. Snowden, *Langmuir*, 2001, **17**, 7145.

11 G. Wakefield, E. Holland, P. J. Dobson and J. L. Hutchison, *Adv. Mater.*, 2001, **13**, 1557.

12 M. Marti, P. Fisher, F. Altorfer, H. J. Sheel and M. Tadin, *J. Phys.: Condens. Matter*, 1994, **6**, 127.

13 D. Lybye, F. W. Poulsen and M. Mogensen, *Solid State Ionics*, 2000, **128**, 91–103.

14 X. Liu and J. Lin, *J. Mater. Chem.*, 2008, **18**, 221–228.

15 X. Liu, R. Pang, Z. Quan, J. Yang and J. Lin, *J. Electrochem. Soc.*, 2007, **154**(7), J185–J189.

16 B. Jacquier, G. Boulon, G. Sallavuard and F. Gaume Mahn, *J. Solid State Chem.*, 1972, **4**, 374–378.

17 A. M. Srivastava, *Mater. Res. Bull.*, 1999, **34**(9), 1391–1396.

18 T. Samuel, C. Satya Kamal, K. Sujatha, V. Veeraiah, Y. Ramakrishana and K. Ramachandra Rao, *Optik*, 2016, **127**, 10575–10587.

19 T. Samuel, C. Satya Kamal, S. Ravipati, B. P. Ajayi, V. Veeraiah, V. Sudarsan and K. Ramachandra Rao, *Opt. Mater.*, 2017, **69**, 230–237.

20 P. Ma, Y. Song, B. Yuan, Y. Sheng, C. Xu, H. Zou and K. Zheng, *Ceram. Int.*, 2017, **43**, 60–70.

21 J. Y. Park, H. C. Jung, G. S. R. Raju, B. Kee Moon, J. Hyun Jeong, S. M. Son and J. Hwan Kim, *Mater. Res. Bull.*, 2010, **45**, 572–575.

22 C. S. Kamal, T. K. Visweswara Rao, P. V. S. S. S. N. Reddy, K. Sujatha, B. P. Ajayi, J. B. Jasinski and K. Ramachandra Rao, *RSC Adv.*, 2017, **7**, 9724.

23 Y. Katayama, H. Kobayashi and S. Tanabe, *Appl. Phys. Express*, 2015, **8**, 012102.

24 V. A. Trepakov, Z. Potucek, M. V. Makarova, A. Dejneka, P. Sazama, L. Jastrabik and Z. Bryknar, *J. Phys.: Condens. Matter*, 2009, **21**, 375303–375308.

25 V. Singh, G. Sivaramaiah, J. L. Rao and S. H. Kim, *Mater. Res. Bull.*, 2014, **60**, 397–400.

26 Z. Han, X. Li, J. Ye, L. Kang, Y. Chen, J. Li and Z. Lin, *J. Am. Ceram. Soc.*, 2015, **98**(8), 2336–2339.

27 R. D. Shannon, *Acta Crystallogr., Sect. A: Cryst. Phys., Diffr., Theor. Gen. Crystallogr.*, 1976, **32**, 751–767.

28 N. V. Chezhina, E. V. Bodritskaya, N. A. Zhuk, V. V. Bannikov, I. R. Shein and A. L. Ivanovskii, *Phys. Solid State*, 2008, **50**, 2121–2126.

29 M. C. Wang, H. J. Lin and T. S. Yang, *J. Alloys Compd.*, 2009, **473**, 394–400.

30 G. Blasse and A. Bril, *J. Inorg. Nucl. Chem.*, 1967, **29**, 266.

31 G. Blasse and B. C. Grabmaier, *Luminescent materials*, Springer-Verlag, Berlin, 1994.

32 P. D. Rack, J. J. Peterson, M. D. Potter and W. Park, *J. Mater. Res.*, 2001, **16**, 1429–1433.

33 M. Grinberg, *Opt. Mater.*, 2002, **9**, 37–45.

34 C. H. Huang, T. W. Kuo and T. M. Chen, *ACS Appl. Mater. Interfaces*, 2010, **2**, 1395.

35 W. H. Di, X. J. Wang, P. F. Zhu and B. J. Chen, *J. Solid State Chem.*, 2007, **180**, 467.

36 G. Blasse, *Phys. Lett. A*, 1968, **28**(42), 444–445.